

Theoretical Modelling of Transport Barriers in Helical Plasmas

S. Toda, K. Itoh, and N. Ohyaabu

National Institute for Fusion Science, Toki 509-5292, Japan

E-mail: toda@nifs.ac.jp

Abstract. A unified transport modelling to explain electron Internal Transport Barriers (e-ITB) in helical plasmas and Internal Diffusion Barriers (IDB) observed in Large Helical Device (LHD) is proposed. The e-ITB can be predicted with the effect of zonal flows to obtain the e-ITB in the low collisional regime when the radial variation of the particle anomalous diffusivity is included. Transport analysis in this article can newly show that the particle fuelling induces the IDB formation when this unified transport modelling is used in the high collisional regime. The density limit for the IDB in helical plasmas is also examined including the effect of the radiation loss.

1. Introduction

The understanding of the turbulence-driven transport and the improved confinement (transport barriers) are the key issue in fusion research. Many kinds of the improved confinement mode in the core plasma of toroidal helical plasmas have been reported; *e.g.*, the e-ITB with the strong positive radial electric field. The radial transition of E_r was predicted to induce the internal transport barrier due to the shear of the radial electric field in the helical plasmas. The transition of E_r was found on the Compact Helical System (CHS), and the improvement of confinement was found inside of the transition point for E_r [1]. Observations on Wendelstein7-AS (W7-AS) [2], LHD [3,4] and the other experiments followed [5]. In the previous study of the e-ITB [6], we have shown the reduction of the heat diffusivity because of the effect of zonal flows, which qualitatively predicts the e-ITB experimentally observed in the whole region of the strong positive E_r . However, we excluded the change of the density profile due to zonal flows effect in the previous study. On the other hand, the IDB in LHD [7] was recently discovered with the strong gradient of the density in a super dense core (SDC) plasma when a series of the pellet is injected. In this article, we present the unified transport model to explain the e-ITB and the IDB. At first, we confirm the reduction of the anomalous diffusivities due to zonal flows when we include the radial variation of the particle anomalous diffusivity in helical plasmas. Next, the theoretical model for the IDB observed in LHD is shown. The mechanism, which is based on the transport reduction due to the shear of the radial electric field, is newly examined in the formation of the IDB. We study the temporal response of the density, the temperatures and the radial electric field to the particle fuelling by the pellet as an initial value problem. It is found that the steepness in the density profile evolves self-generatedly. After the pellet ablation, the shear of the radial electric field increases and the associated reduction of the particle diffusivity is obtained. The jump of the particle diffusivity at the radial transition point of the improved confinement region gets steeper after the pellet fuelling. To study the physics of the transport barrier, the investigation of the density limit including the radiation loss for the case of the IDB in LHD is necessary. We show the dependence of the electron temperature on the electron heating in the case of the IDB in helical toroidal plasmas when the effect of the radiative loss is included in a set of the transport equations.

2. One-dimensional model for transport equations

The one-dimensional transport model is employed. The cylindrical coordinate is used and r -axis is taken in the radial cylindrical plasma in this article. The region $0 < \rho < 1$ is considered, where a is the minor radius and $\rho = r/a$. The temporal equations for the density (

n) and the temperatures the electron temperature (T_e) and the hydrogen ion temperature (T_i) in this article are same as those given in [6]. The expression for the radial neoclassical flux associated with helical-ripple trapped particles Γ_j^{an} for the species j . In the case of the analysis about the e-ITB, the form which was given in [8] is used in this article. This form covers from the v_j regime to the $1/v_j$ regime, where v_j is the collision frequency. In the case of the calculation about the IDB with the high density plasma, we use the form for the radial neoclassical flux given in [9], which is available in the Pfirsch-Schlüter regime, because the plasma state of the IDB/SDC plasma corresponds to the high collisional regime. In the temporal equation for the density, the term S_n , which represents the particle source, is used. The quantity S_p is the modelled particle source of the pellet fuelling in the case of the analysis about the IDB. (In the calculation about e-ITB, $S_p=0$.) In the equations for the electron and ion temperatures, the term P_{he} represents the absorbed power due to the electron cyclotron resonance heating (ECRH) and the term P_{hi} represents the absorbed power of ions, respectively. In the temporal equations of the density and temperatures, we use the turbulent particle diffusivity D_T and the turbulent heat diffusivity χ_T . A theoretical model for the turbulent diffusivity is adopted.

In the case of the analysis about the IDB, we use the ambipolar condition $\Gamma_i^{\text{an}} = \Gamma_e^{\text{an}}$ with the hydrogen plasma to determine the radial profile of the electric field. On the other hand, in the case of the calculation about zonal flows, the temporal equation for the radial electric field in a nonaxisymmetric system [10] is analyzed in the same system of the temporal transport equations given in [6].

The equations of density, temperature and electric field are solved coupled under the appropriate boundary conditions. We fix the boundary condition at the center of the plasma ($\rho=0$) such that $n'=T_e'=T_i'=E_r=0$. For the diffusion equation of the radial electric field, the boundary condition at the edge ($\rho=1$) is chosen as $\Gamma_i^{\text{an}} = \Gamma_e^{\text{an}}$. The boundary conditions at the edge ($\rho=1$), with respect to the density and temperature, are given by specifying the gradient scale lengths. We employ those expected in LHD: $-n/n'=0.1\text{m}$, $-T_e'/T_e = -T_i'/T_i = 0.1\text{m}$ in this article. The machine parameters which are similar to those of LHD are set to be $R = 3.6\text{m}$, $a = 0.6\text{m}$, $B = 3\text{T}$, $\ell = 2$ and $m = 10$. In this article, we set the safety factor and the helical ripple coefficient as $q = 1/(0.4 + 1.2\rho^2)$ and $\epsilon_h = 2\sqrt{1 - (2/(mq(0)) - 1)I_2(mr/R)}$, respectively. Here, $q(0)$ is the value of the safety factor at $\rho=0$ and I_2 is the second-order modified Bessel function.

3. Model of turbulent transport coefficients

We adopt the model for the turbulent heat diffusivity χ_a based on the theory of the self-sustained turbulence due to the interchange mode [11] and the ballooning mode [12], both driven by the current diffusivity. The anomalous transport coefficient for the temperatures is given as $\chi_a = \chi_0 / (1 + G\omega_{\text{El}}^2)$ ($\chi_0 = F(s, \alpha)\alpha^{3/2}c^2v_A / (\omega_{\text{pe}}^2 qR)$), where ω_{pe} is the electron plasma frequency. The factor $F(s, \alpha)$ is the function of the magnetic shear s and the normalized pressure gradient α . The parameter ω_{El} represents the effect of the reduction of the anomalous transport due to the shearing rate of the radial electric field. The details about the parameters F and G were given in [11,12].

In the analysis about the e-ITB, we introduce the effect of zonal flows (ZFs) to the turbulent diffusivities, because ZFs are predicted to be excited due to the strong positive electric field in the parameter regime where the e-ITB is observed. Zonal flows (at nearly zero frequency) are generated by the fluctuations and strongly influence the turbulent transport. The damping rate

of ZFs, v_{damp} , controls the turbulent transport. The damping of ZFs is caused by the collisional process and by the self-nonlinearity of ZFs [13]. Whether zonal flows are excited or not is judged by comparing χ_a (which is given in the absence of zonal flows) with the quantity $\chi_{\text{damp}} \equiv k_{\perp}^2 q_r^{-2} k_{\theta}^{-2} v_{\text{damp}}$, where q_r is the wave number of zonal flows, k_{θ} is the poloidal wave number and k_{\perp} are the perpendicular wave number of the microscopic fluctuations, respectively. To determine the value of the turbulent diffusivity χ_T with the effect of ZFs in the transport codes, the same procedure in [6,14,15] is used. Owing to the dependence of v_{damp} on E_r , the damping rate of ZFs: v_{damp} is small in the electron root branch of e-ITB (i.e., the strong positive E_r). The turbulent transport coefficient becomes smaller when the strong positive radial electric field is established in e-ITB [15], when we consider the role of ZFs in the e-ITB formation in helical plasmas. The value for the turbulent diffusivities of the particle is set as $D_T = \chi_T$ to include the radial variation of the density profile. We also set $D_{\text{ET}} = \chi_T$ in order to examine the typical length for the electric field shear at the transition point, where D_{ET} is the diffusion coefficient with respect to the radial electric field.

As a strong positive electric field cannot be obtained in the parameter regime of IDB/SDC plasmas, no significant reduction of the diffusivities is predicted due to the effect of ZFs. Therefore, we set $\chi_T = \chi_a$. The value for the anomalous diffusivities of the particle is set as $D_T = \chi_T$ to examine the radial variation in the profile of the particle diffusivity D_T when the steep radial gradient in the density profile can be obtained as a calculation result.

4. Model of particle and heat sources

In the case of the analysis about the e-ITB plasmas, the particle source S_n is set to be $S_n = S_0 \exp((r-a)/L_0)$. This profile represents the peaking at the plasma edge of the particle source due to the ionization effect. The coefficient S_0 is chosen as $3 \times 10^{22} \text{m}^{-3} \text{s}^{-1}$ and L_0 is set to be 0.1m. The intensity S_0 governs the average density, and is taken as a control parameter to specify the density in this article. The radial profiles of the electron and ion heating terms, P_{he} and P_{hi} , are assumed to be proportional to $\exp(-(r/(0.2a))^2)$ for the sake of the analytic insight.

In the case of the calculation about IDB/SDC plasmas, we introduce the term S_p of the additional particle source to the temporal equation of the density in order to examine the effect of the pellet injection. This parameter S_p has a distribution as $S_p = S_{p0} \exp(-(r/r_p)^2)$ and is set to have a value from the initial time $t=0$ to 1ms. In other words, we set as $S_{p0} = 1 \times 10^{23} \text{m}^{-3} \text{s}^{-1}$ for $0 < t \leq 1\text{ms}$ and $S_{p0} = 0 \text{m}^{-3} \text{s}^{-1}$ for $t > 1\text{ms}$. We set the half width of the profile S_p as $r_p = 0.2a$. To establish the target plasma, the particle source term S_n is also set to be $S_n = S_0 \exp((r-a)/L_0)$. Here the coefficient S_0 is taken as $7 \times 10^{20} \text{m}^{-3} \text{s}^{-1}$ and L_0 is set to be 0.1m. This particle source is chosen to obtain a self-consistent steady plasma which are used as the initial condition of the next calculation including the effect of the particle fuelling (particle injection). In both cases, the absorbed power of electrons is set to be 1MW and the absorbed power of ions is taken as 0MW, respectively. The radial profiles of the electron and ion terms of the absorbed powers, P_{he} and P_{hi} , are set to be proportional to $\exp(-(r/(0.5a))^2)$.

5. Results of the analysis about e-ITB plasmas

The bifurcation of E_r itself induces the transition of the turbulent transport in the bulk of the plasma column as well as at the shear of the electric field. The dependence of χ_T on the

damping rate of ZFs, explains the improved confinement in the e-ITB region of toroidal helical plasmas. The reduction of the turbulent transport in the entire region of the strong positive E_r is demonstrated with the effect of the radial variation of the particle diffusivity. The one-dimensional transport analysis for LHD-like plasma has been performed and the radial profiles of E_r , T_e , T_i and n are solved. In this analysis, the total thermal diffusivity is given as the sum of χ_T and neoclassical transport. An example is taken from the plasma, which is sustained by ECRH. In order to set the line-averaged temperature of electrons to be around $\bar{T}_e = 1.1\text{keV}$ (T_e at the center, $T_e(0) = 2.6\text{keV}$) and the line-averaged density to be around $\bar{n} = 2 \times 10^{19}\text{m}^{-3}$ for the choice of the above mentioned anomalous transport coefficients. The line-averaged ion temperature is chosen to be about $\bar{T}_i = 0.6\text{keV}$ ($T_i(0) = 0.9\text{keV}$). When we evaluate χ_{damp} , we employ an estimate $k_{\perp}^2 q_r^{-2} k_{\theta}^{-2} \rho_i^{-2} \sim 50$ [15]. In this parameter regime examined here, we obtain the strong positive E_r in the core region: $E_r \cong 15(\text{kV/m})$.

A profile of the anomalous heat diffusivity with the zonal flow effect (solid line) is shown in FIG. 1. In both cases with and without the effect of ZFs, the radial transition of E_r from the positive one to the negative one can be shown. The radial point for the steepest gradient of E_r is defined by the parameter ρ_T . The clear reduction of the anomalous diffusivity with ZFs effect is shown in the core region compared with that without ZFs effect. In the calculation here, we take the radial variation of the particle diffusivity. The value of the density becomes larger due to the reduction of the particle diffusivity with the effect of ZFs compared with that without the effect of ZFs when we take the same value for S_0 . Therefore, the value with ZFs effect of the radial point for E_r transition: ρ_T is different from that without ZFs. The radial point of ρ_T moves inside if the effect of ZFs is included in this calculation. The reduction of the total heat diffusivities with the effect of ZFs can be examined compared with those without the effect of ZFs. The value of the reduced transport coefficient is close to what has been reported from LHD experiments [16]. The damping rate of ZFs is small in the electron root branch. The turbulent transport coefficient becomes smaller when the strong positive radial electric field is formed. Outside the transition point ρ_T , where the ion root branch appears, the damping rate becomes large and the strong zonal flows are not excited. Thus, the reduction is not expected for the region $\rho > \rho_T$ in this example.

The excitation of ZFs strongly depends on the plasma wave number because whether ZFs are excited or not is judged by comparing χ_a with the quantity $\chi_{\text{damp}} \cong k_{\perp}^2 q_r^{-2} k_{\theta}^{-2} v_{\text{damp}}$. The value of $k_{\perp}^2 q_r^{-2} k_{\theta}^{-2} \rho_i^{-2} \sim 50$ ($k_{\perp}^2 q_r^{-2} \sim 6$, $k_{\theta} \rho_i \sim 1/3$) is chosen in this calculation. If the value of $k_{\theta} \rho_i$ becomes large, the value of the criterion χ_{damp} for the excitation for ZFs decreases if the value of $k_{\perp} q_r$ is fixed. In this case, ZFs tend to be excited. At that time, the anomalous transport will be reduced further.

6. Results of the analysis about IDB/SDC plasmas

One-dimensional transport analysis for the LHD-like plasma is performed, using the models of the particle and heating sources shown in Sec. 4. The temporal response to the plasma due to the additional particle source is studied. The dynamics of the plasma radial profiles for (a) the density, (b) the electron temperature, (c) the ion temperature and (d) the radial electric field at the times 0ms, 1ms and 10ms is shown in FIG. 2. The profiles labeled by 0ms represent the initial stationary

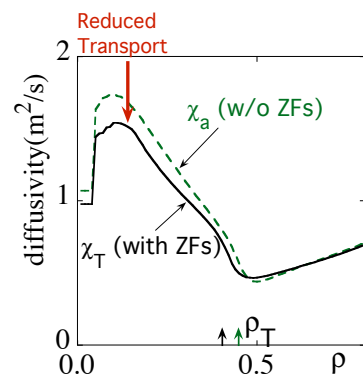


FIG.1 Reduction of the anomalous heat diffusivity due to the effect of zonal flows.

state used in the calculation. The profiles are shown, with the dashed lines in FIG. 2, at the time 1ms when the pulse of the additional particle source S_p is switched off. The solid lines in FIG. 2 show the profiles at the time 10ms, illustrating the self-generated dynamics. The temporal increase of the density at the time 1ms from the initial condition in the core region, which is caused by the additional particle source S_p , is shown in FIG. 2(a). After the time 1ms, the density in the core region continues to increase slightly because there is an inward neoclassical transport due to the positive gradient of the temperature profiles. The sharp change of the gradient in the density profile at 10ms can be found. The profiles of the electron and ion temperature are shown in FIG. 2(b) and (c), respectively. The temperatures in the core region decrease from the initial condition because the density in the core region increases by the additional particle source and the pressure is constant in this time scale (~ 1 ms), which is shorter than the confinement time (~ 1 s). The gradient of ion temperature becomes smaller especially in the effective region of the additional particle fuelling S_p . At the end of the additional particle source (1ms), the gradient of E_r is steeper (the dashed line in FIG. 2(d)) owing to the effect of the additional particle source S_p . We emphasize the much steeper gradient of the radial electric field at the transition point ρ_T in FIG. 2(d) is generated at the time 10ms. The parameter ρ_T represents the location of the steepest gradient of E_r at 10ms in FIG. 2(d). The gradient of the radial electric field is strong to suppress the anomalous transport: $E_r' \cong 1 \times 10^5 \text{ Vm}^{-2}$ at $\rho = \rho_T$. Therefore, the improvement near the transition point is induced. A profile of the anomalous transport diffusivity is shown in FIG. 3 at $t = 10$ ms with the solid line. A clear reduction of the anomalous particle diffusivity is found at the transition point $\rho = \rho_T$ due to the strong gradient of E_r compared with the region $\rho > \rho_T$ at the time 10ms. We confirm that the value of the anomalous particle diffusivity is much larger than that of the neoclassical particle diffusivity in the region $\rho < 0.4$ in the parameter region examined here. At the time 10ms, the value of the anomalous particle diffusivity decreases in the region $\rho < \rho_T$, while the value of the anomalous particle diffusivity increases $\rho > \rho_T$ compared with those of the anomalous particle diffusivity at the time 1ms. We can make the self-generated barrier clear at the time 10ms in the radial profile of the anomalous particle diffusivity. Therefore, the barrier with respect to the particle transport in the density profile can be obtained in FIG. 2(a) at 10ms.

The mechanism why the gradient of E_r becomes steeper after the additional particle fuelling is switched off is as follows. The value of E_r which is given by the solution of the ambipolar condition is approximately written as $E_r = T_i(n'/n + C_i T_i'/T_i)/e$, where $C_i \cong 3$ in the parameter region of $n \geq 1 \times 10^{20} \text{ m}^{-3}$ and $T_e \approx T_i$. Note that the contributions to E_r from the gradient of T_i are stronger than that from the gradient of n by the factor C_i . Owing to the effect of the additional particle source S_p , the value of E_r' changes. At the time 1ms, the

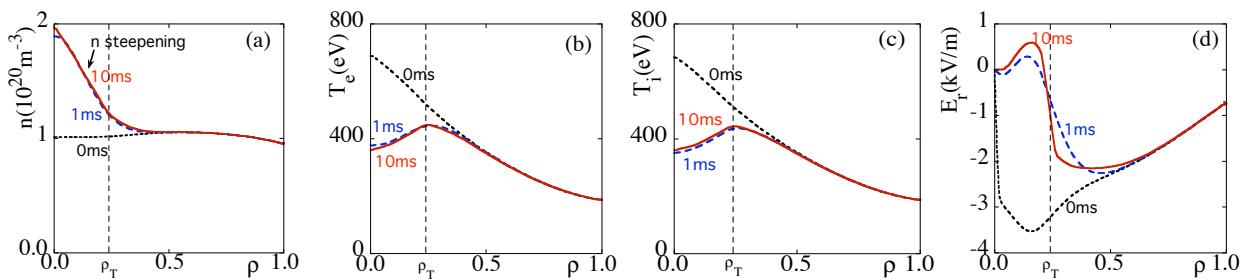


FIG. 2 The dynamics of the radial profiles of (a) the density, (b) the electron temperature, (c) the ion temperature and (d) the radial electric field. The dotted line, the dashed line and the solid line show the states at the times 0ms, 1ms and 10ms, respectively.

gradient of the radial electric field is obtained to some extent because the value of T_i decreases in the effective region of the additional particle fuelling S_p . Next, we examine the self-generated dynamics of E_r' . From the time 1ms to the time 10ms in the region $\rho < \rho_T$, the density gradient slightly decreases and the gradient of the ion temperature increases, respectively. Because the contribution from the gradient of the ion temperature to the ambipolar equation dominates the contribution from the gradient of the density, the value of the radial electric field becomes larger at the time 10ms than that at the time 1ms in the region $\rho < \rho_T$. From the time 1ms to the time 10ms in the region $\rho > \rho_T$, the density gradient slightly increases and the gradient of the ion temperature decreases, respectively. Thus, the value of the radial electric field becomes smaller at the time 10ms than that at the time 1ms in the region $\rho > \rho_T$. Thus, the strong shear of the radial electric field is self-organized at the transition point $\rho = \rho_T$, after the additional particle source is switched off. When the strong shear of E_r appears, the anomalous particle diffusivity is reduced and the gradient of the temperature gets steeper. As the results, the gradient of the radial electric field is found to be self-generatedly much steeper.

It is emphasized that the barrier formation continues after the additional particle source is switched off. The reduction of the anomalous transport is much clearer in the region $\rho < \rho_T$ after the additional particle source is switched off (10ms) than the case at the time 1ms. Whether we can obtain the strong shear of the radial electric field depends on the amount of the additional particle source. In this case $S_{p0} = 1 \times 10^{23} \text{ m}^{-3} \text{ s}^{-1}$, the strong gradient of E_r to reduce the anomalous transport evolves as self-organized and we show that the typical time scale to obtain the strong gradient of E_r is around 10ms in the parameter regime examined here. If we set much smaller value for S_p , $S_{p0} = 2 \times 10^{22} \text{ m}^{-3} \text{ s}^{-1}$, the gradient of E_r increases by the additional particle source at $t = 1\text{ms}$. However, the gradient of E_r smoothly decreases and the state returns to the initial one. This suggests that there is the threshold value of the S_{p0} in the dependence of the shear of the radial electric field.

The bifurcation nature in the plasma dynamics is studied. The dependence of E_r' on the magnitude of the particle fuelling S_{p0} is shown in FIG. 4 at the times: $t = 1\text{ms}$ (open triangle marks) and $t = 10\text{ms}$ (closed circle marks). The continuous change of E_r' is shown at the time 1ms in FIG. 4. At the time 10ms, the sharp change of E_r' due to the additional particle source clearly demonstrates around $S_p = 5 \times 10^{22} \text{ m}^{-3} \text{ s}^{-1}$. Threshold value for S_p , $S_{p\text{th}} \cong 5 \times 10^{22} \text{ m}^{-3} \text{ s}^{-1}$ can be found. In the case $S_p < S_{p\text{th}}$, the state returns to the initial state which has no transport improvements after the additional particle source is switched off. If the value of S_{p0} becomes larger and the relation $S_p > S_{p\text{th}}$ satisfies, we can find the self-generated shear of the radial electric field in the plasma dynamics after the additional particle source is switched off. At the time 10ms, the shear of the radial electric field gets steeper, following the relation

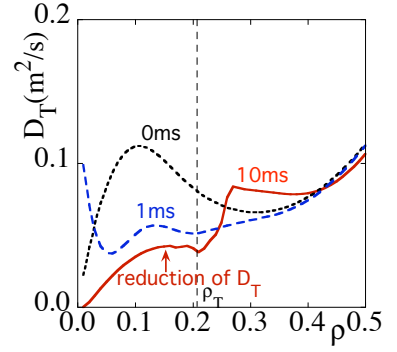


FIG. 3 The radial profiles of the anomalous particle diffusivity D_T in the region $0 < \rho < 0.5$ at the times 0ms (dotted line), 1ms (dashed line) and 10ms (solid line).

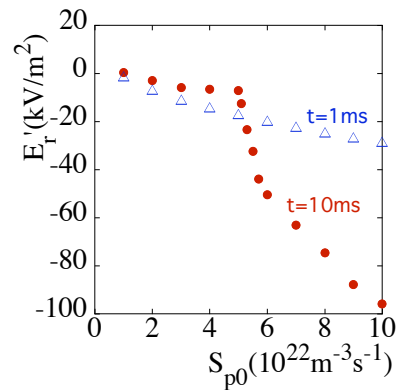


FIG. 4 The dependence of the radial electric field shear in a region $0.15 < \rho < 0.25$ at $t = 10\text{ms}$ and at $t = 1\text{ms}$ on the particle fuelling S_{p0}

$E_r'(S_{p0}) - E_r'(S_{pth}) \propto -(S_{p0} - S_{pth})^{0.43 \pm 0.10}$ in the region $S_p > S_{pth}$. This sharp change of E_r' depending on the additional particle source demonstrates the bifurcation nature in the plasma dynamics.

7. Study of the Density Limit for the IDB

To examine the density limit for the thermal stability in the case of the IDB, we add the term of the radiation loss rate of the energy to the temporal equation of the electron temperature. The combined mechanism of the transport and the radiation loss of the energy are discussed. The form of the radiative loss rate was given in [17]. As an example, we take a carbon plasma with $n_{\text{carbon}} = 0.01n$, where n_{carbon} is the density of the carbon. For simplicity, the density profile from [7] is used for the IDB plasma as the temporally fixed density profile in the calculation here. We examine the temporal evolutions of the electron and ion temperatures, and the profile of the radial electric field from the ambipolar condition. The profiles of the electron temperature are shown in FIG. 5 with two cases of the electron heating in the region $0.8 < \rho < 1.0$. The solid line and the dashed line represent the case that the electron heating is 1.28MW and 1.29MW, respectively. In the case that the electron heating is 1.28MW, the sharp decrease of the electron temperature is shown near the edge. This is because the increase of the radiative loss rate at the low temperature ($T_e < 10\text{eV}$).

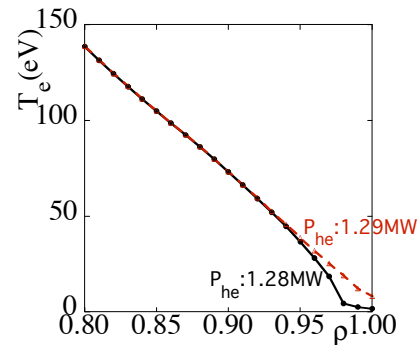


FIG. 5 The radial profile of the electron temperature with the effect of the radiative cooling loss.

8. Summary

The unified transport modelling is done with respect to the dynamics and the radial structure of profiles of the density, the temperatures and the electric field in toroidal helical plasmas. The analysis is performed by use of the one-dimensional transport equations. At first, we have studied the role of zonal flows in the e-ITB formation of toroidal helical plasmas with the radial variation of the particle diffusivity. The reduced damping of zonal flows which causes the suppression of the turbulent transport is confirmed. The results of the transport code analysis show that the total heat diffusivity in the entire inner region is reduced. The effect of zonal flows on the anomalous transport is investigated. The transport reduction is obtained in the wide region in conjunction with the e-ITB. This is the demonstration that the change of the collisional damping of zonal flows can cause the transition in the turbulent transport. Next, the temporal response of the plasma in the presence of the additional particle fuelling was studied related with IDB/SDC plasmas observed in LHD. After the particle ablation, the gradient of the radial electric field is self-generated to get steeper owing to the plasma transport. The particle transport continues to reduce after the particle fuelling in the region $\rho < \rho_T$ due to the shear of the electric field. Thus, the reduction of the anomalous particle diffusivity across the transition point ρ_T at $t = 10\text{ms}$ becomes clearer than that at the end of the particle fuelling (1ms). It is found that there is a threshold of the particle fuelling (the pellet size in the experiment) to establish the barrier in the density profile. The typical time scale is shown to obtain the reduction of the particle anomalous diffusivity. This prediction may be the theoretical explanation for the IDB/SDC plasmas in LHD [7]. The dependence of the electron temperature on the electron heating was studied in the case of the IDB/SDC plasmas with the radiative loss. The threshold value of S_p for IDB plasmas strongly depends on the shape of the distribution. To study the threshold value of S_p to obtain the barrier of the

particle transport, the parameter survey of the calculations results is necessary. The study of the other case of the duration for the particle fuelling is planned. We will study the dependence of the critical density on the power input in the presence of the radiative loss in helical plasmas. These are left for future studies.

The authors would like to acknowledge Prof. A. Fukuyama for the helpful suggestions related with the numerical methods. This work is partly supported by a Grant-in-Aid of JSPS (No. 19360418), a Grand-in-Aid for the Specially-Promoted Research of MEXT (No. 16002005) and the NIFS Collaborative Research Programs, NIFS08KLDD014 and NIFS08KNXN122.

References

- [1] FUJISAWA, A., et al., “Electron Thermal Transport Barrier and Density Fluctuation Reduction in a Toroidal Helical Plasma”, *Phys. Rev. Lett.* **82** (1999) 2669.
- [2] STROUTH, U., et al., “Internal Transport Barrier Triggered by Neoclassical Transport in W7-AS”, *Phys. Rev. Lett.* **86** (2001) 5910.
- [3] IDA, K., et al., “Characteristics of Electron Heat Transport of Plasma with an Electron Internal-Transport Barrier in the Large Helical Device”, *Phys. Rev. Lett.* **91** (2003) 085003.
- [4] SHIMOZUMA, T., et al., “Formation of electron internal transport barriers by highly localized electron cyclotron resonance heating in the large helical device”, *Plasma Phys. Control. Fusion* **45** (2003) 1183.
- [5] FUJISAWA, A., “Experimental studies of structural bifurcation in stellarator plasmas”, *Plasma Phys. Control. Fusion* **45** (2003) R1.
- [6] TODA, S. and ITOH, K., “Transport analysis of the effect of zonal flows on electron internal transport barriers in toroidal helical plasmas”, *Nucl. Fusion* **47** (2007) 914.
- [7] OHYABU, N., et al., “Observation of Stable Superdense Core Plasmas in the Large Helical Device”, *Phys. Rev. Lett.* **97** (2006) 055002.
- [8] SHAING, K. C., “Stability of the radial electric field in a nonaxisymmetric torus”, *Phys. Fluids* **27** (1984) 1567.
- [9] SHAING, K. C. and CALLEN, J. D. “Neoclassical flows and transport in nonaxisymmetric toroidal plasmas”, *Phys. Fluids* **26** (1983) 3315.
- [10] HASTINGS, D. E., “A differential equation for the ambipolar electric field in a multiple-helicity torsatron”, *Phys. Fluids* **28** (1985) 334.
- [11] ITOH, K., et al., “Confinement improvement in H-mode-like plasmas in helical systems”, *Plasma Phys. Control. Fusion* **36** (1994) 123.
- [12] ITOH, K., et al., “Self-sustained turbulence and L-mode confinement in toroidal plasmas. I”, *Plasma Phys. Control. Fusion* **36** (1994) 279.
- [13] DIAMOND, P. H., et al., “Zonal flows in plasma—a review”, *Plasma Phys. Control. Fusion* **47** (2005) R35.
- [14] ITOH, K., et al., “Coherent structure of zonal flow and onset of turbulent transport”, *Phys. Plasmas* **12** (2005) 062303.
- [15] ITOH, K., et al., “Physics of internal transport barrier of toroidal helical plasmas”, *Phys. Plasmas* **14** (2007) 020702.
- [16] MOTOJIMA, O. et al., “Overview of confinement and MHD stability in the Large Helical Device”, *Nucl. Fusion* **45** (2005) S255.
- [17] POST, D. E., et al., “Steady-State Radiative Cooling of Low-Density High-Temperature Plasmas”, *Atomic Data and Nuclear Data Tables* **20** (1977) 397.